Pollution, 5(2): 301-312, Spring 2019
DOI: 10.22059/poll.2018.266785.526
Print ISSN: 2383-451X Online ISSN: 2383-4501
Web Page: https://jpoll.ut.ac.ir, Email: jpoll@ut.ac.ir

Simulating the Influence of Greenhouse Gases on the Climate of West Africa

Adeniyi, M. O.*, Nymphas, E. F. and Oladiran, E. O.

Department of Physics, University of Ibadan, P.O. Box 22133, Ibadan, Nigeria

Received: 04.10.2018 Accepted: 15.01.2019

ABSTRACT: The response of climate to perturbations in GHGs is location dependent. Six experiments: control (CTRL); double CH_4; double CO_2; double N_2O; halved CFC11 and halved CFC12 were carried out to reveal the local area response to different GHGs levels in the atmosphere over West Africa. Double CH_4, CO_2 and N_2O generally induce wetness but they also induce localized dryness at the hilly and mountainous areas of SW Ghana, Central Nigeria, Northern Cameroon and South-eastern Central African Republic. Increase in ground temperature is induced by double GHGs with intensified warming at the north by double CO_2. However, patches of cooling are induced at the north. Changes in specific humidity induced by double CO_2, CH_4 and N_2O are similar. Intensified tropical easterly jet is induced by double GHGs. A dipole anomaly of wind with positive at the lower latitude and negative at higher latitude is induced at the northern part of West Africa. Significant reduction in cloud water content is induced from 900 to 400 hPa and 0 and 15^{o}N.

Keywords: Cooling; warming, induced dryness; induced wetness.

INTRODUCTION

Influence of aerosols and Greenhouse Gases (GHGs) on climate is a function of the response of the climate parameters in a particular location and this depends on the geographical built-up of the location (Lin et al., 1988; Baede et al., 2001; Berntsen, 2006; Strangeways, 2011). The influence on climate will in turn influence the environment, health of man and animal and the ecology of such environment (McMichael, 2001; Watson et al., 2001). The influence is better studied using dynamical models either General Circulation Models (GCMs) or Regional Climate Models (RCMs). Stainforth et al. (2007) revealed the uncertainties associated with climate prediction. However, based on improved modelling techniques in recent time, Anderson et al. (2016) reported the reliability of 21st century projection by earth system models and the expected continuous warming in response to CO_2 emissions. Other causes of global warming have also been highlighted (Hansen, 2013)

The GHGs are abundant in the following order: water vapour (H_2O); Carbon dioxide (CO_2); Methane (CH_4); Nitrous oxide (N_2O); ozone (O_3); Chlorofluorocarbons (CFCs) and Hydrofluorocarbons (HCFCs and HFCs) (Karl & Tremberth, 2003; Le Treut et al., 2007). The greenhouse impact of each of the gases depends on its abundance, not necessarily its potential for greenhouse effect. Attempt to increase agricultural productivity through cultivation of more rice paddy, tillage and use of fertilizers has

* Corresponding Author Email: mojisolaadeniyi@yahoo.com; Tel: +2348033579081

led to more increase in CH_4 and N_2O emissions (Bousquet et al., 2006). Moreover, the primary GHGs also combine with pollutants in the atmosphere to form other GHGs such as ozone (Ramanathan & Feng, 2009). Etminan et al. (2016) reported 25% increase CH_4 contributions to warming with respect to previous estimate, the reported increase in potential of CH_4 to increase global warming is due to its ability to absorb radiation at shorter wavelength in the lower atmosphere. This factor is not included in the previous analysis of warming effect of CH_4. Previously, CH_4 and N_2O have higher potential for global warming in multiples of 25 and 298 of CO_2 potential for global warming (Zhang et al., 2013). Zaehle et al. (2011) revealed the double impact of N_2O on climate, when nitrogen is used to improve soil fertility; it increases the rate of CO_2 absorption from the atmosphere by the ecosystem. The global warming effect of CO_2 is then reduced. On the other hand, more nitrogen in the soil will lead to emission of more N_2O which has higher potential for global warming than CO_2.

Most studies have been on the global abundance and impact of GHGs on the environment (Zaehle et al., 2011; Davidson & Kanter, 2014; Etminan et al., 2016); only a few have studied the impact of GHGs on the environment at local and regional scales. Zhuang et al. (2007) studied the CH_4 and CO_2 emission and their implications for Alaska regional GHG budget. Zhang et al. (2013) also studied the influence of different tillage system on CH_4 and CO_2 emission from a double cropped paddy in Southern China. The influence of changes in GHG concentration on the climate depends on the sensitivity of climate to such changes at such areas (Berntsen, 2006; Lin et al., 1988). The influence of the individual GHGs over the local and regional parts of West Africa is yet to be documented. It is important to know how the GHG emissions will affect the climate and ecosystem at the study area, since the economy of most West African countries is being diversified towards agriculture (Suberu et al., 2015; Adams, 2016). This paper aims at simulating the impact of changes in GHGs concentration in the atmosphere on the climate of West Africa, using the version 4.5 of the International Centre for Theoretical Physics (ICTP) Regional Climate Model (RegCM4.5).

MATERIALS AND METHODS

The RegCM4.5 was employed in this work. The dynamical core of the model is of two types: hydrostatic and non-hydrostatic. The hydrostatic core was used for the six experiments carried out in this study. The details of the experimental setup used for this study are shown in Table 1. The same domain and experimental set up was used for the six simulations (Fig. 1). The domain consists of 120 x 100 horizontal grids centred on longitude 0.0 ^oE and latitude 12.5 ^oN. In addition to the general experimental set up (Table 1) for the six experiments; the control simulation contains six greenhouse gases in the normal proportion(A1B scenario), the $CO_2$2 experiment contains double CO_2, N_2O2 experiment contains double N_2O, $CH_4$2 experiment contains double CH_4 while CFC110.5 and CFC120.5 experiments contain half CFC11 and CFC12, respectively. The double greenhouse gases experiments also contain the other gases in the normal proportion (A1B scenario) and are done with increased 1.5^oC air temperature and Sea Surface Temperature (SST). All the experiments are initiated at 01 June, 2002 and end at 01 October, 2002.The first month is used as spin up.

Table 1. Experimental set up and boundary conditions in Regional Climate Models version 4.5 used in this study.

Dynamics	Hydrostatic core
Model domain centre	longitude 0.0 ^{o}E and latitude 12.5 ^{o}N; resolution=50 km
Map projection	Mercator
Topography data	Global 30 Arc-Second Elevation topography dataset.
Vertical coordinate	23 sigma levels
Planetary boundary layer	Holtslag et al. (1990)
Cumulus parameterization	Grell with Arakawa-Schubert closure on land and Emanuel on ocean (Arakawa & Schubert, 1974; Emanuel, 1991)
Microphysics parameterization	Subgrid Explicit Moisture Scheme (SUBEX; Pal et al., 2000).
Land surface scheme	Biosphere-Atmosphere Transfer Scheme (BATS)
Radiation parameterization	The National Center for Atmospheric Research (NCAR), Community Climate System Model (CCM3) (Kiehl et al.,1998)
Ocean flux parameterization	Zeng et al. (1998)
The time step Initial and lateral boundary	2.5 minutes
conditions	Era Interim 1.5 Reanalysis data sets (Dee et al., 2011)
Oceanic boundary condition	Six hourly updated, Optimum Interpolated (OI) SST weekly SST data

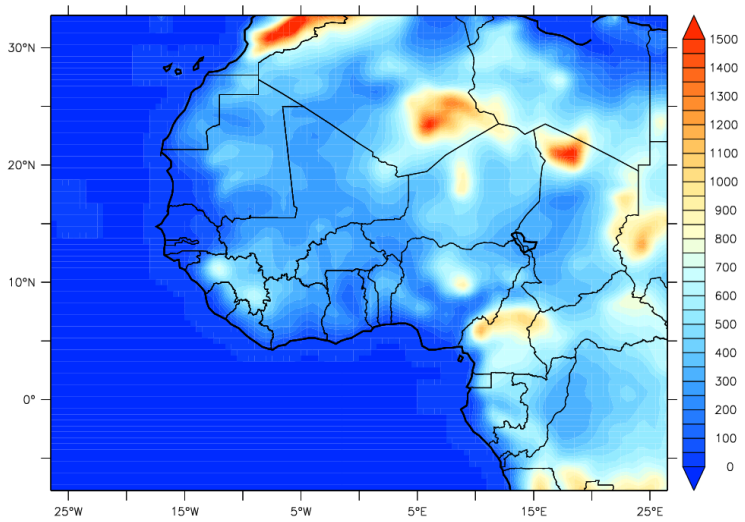

Fig. 1a. Topography (m) of the domain of simulation. The vertical axis represents the latitude while the horizontal axis is the longitude.

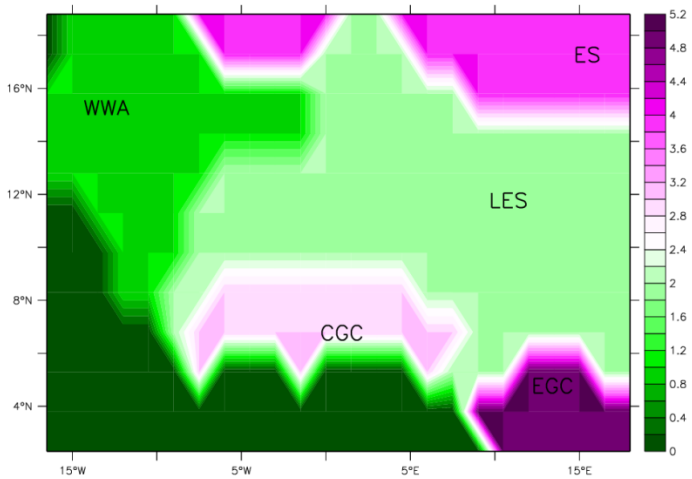

Fig. 1b. Five regions of precipitation delineated by Adeniyi (2016). WWA is Western West Africa, ES is Eastern Sahel, LES is Lower Eastern Sahel, CGC is Central Guinea Coast and EGC is Eastern Guinea Coast. The vertical axis represents the latitude while the horizontal axis is the longitude.

RESULTS AND DISCUSSION

Simulated precipitation (mm/day) from the control experiment is shown in Fig. 2a with precipitation greater than 1 mm day^{-1}generally between 5 and 15^{o}N and higher precipitation at the lower part of Western West Africa (WWA) precipitation region (Fig. 1b) where there are mountains, highlands and ocean (Adeniyi, 2014; 2016). The $CH_4$2 induced precipitation is generally higher than the control over the ocean and the coast (Fig. 2b). The increase in precipitation has a spatial coverage between 5 and 12^{o}N with more wetness at the lower part of WWA and Lower Eastern Sahel (LES, Fig. 1b). However, dryness prevails in some areas such as 10^{o}N between -5 and 10^{o}E (lower part of LES), and the south-eastern part of the simulation domain (Fig. 2b). There is little or no change in simulated precipitation at the northern part of the simulation domain (14-33^{o}N), where the control simulated precipitation is less than 1 mm/day. Similar spatial pattern of $CO_2$2 induced precipitation is simulated with spatial spread of precipitation increase with respect to the changes induced by $CH_4$2 (Fig. 2b, c). Stronger dryness with respect to $CH_4$2 induced dryness prevails between 0 and 15^{o}E at around 10^{o}N. The N_2O2 also induced a similar spatial precipitation changes over West Africa with intensified and spatial spread of wetness over land. The relatively intensified and spatial spread of induced wetness reveals the higher potential of N_2O for global warming despite its low abundance (Zaehle et al. 2011). Relatively reduced spatial spread of dryness is induced by N_2O2 over land except at the south-eastern part of the simulation domain (Fig. 2d). Wetter West Africa caused by $CH_4$2, $CO_2$2, and N_2O2 corroborates the warming effect of GHGs, but the dryness induced in some areas supports the area dependent nature of GHGs effect on climate (Berntsen, 2006; Lin et al., 1988). The CFC110.5 experiment induced similar changes in precipitation. Noticeable reduction in precipitation is simulated only at 10^{o}N, from -13 to 10^{o}E. The induced precipitation changes simulated by CFC120.5 are similar to CFC110.5 simulation (Fig. 2e, f). Since CFC110.5 and CFC120.5 are experiments that reduce the level of GHGs in the atmosphere, the simulated reduction in precipitation is expected. The simulated induced wetness from the CFC110.5 and CFC120.5 is also not strange as a result of the presence of CO_2, CH_4 and N_2O in the atmosphere based on A1B scenario. The area with induced dryness (10^{o}N, from -13 to 10^{o}E; Ivory Coast, Northern Sierra Leone, South eastern Guinea and central Nigeria) are generally hilly and mountainous areas. The dryness that prevailed at the hilly and mountainous areas is probably as a result of lower precipitation than evaporation which leads to drought.

Figure 3 shows the simulated ground temperature from the control and greenhouse gases experiments. Simulated ground temperature is high at the northern part of the simulation domain (LES and Eastern Sahel (ES), Fig. 1b) compared to the southern part (lower WWA, Central Guinea Coast (CGC) and Eastern Guinea Coast (EGC), Fig. 1b). It is relatively low at the mountains (Cameroon, Guinea, Sierra Leone, Liberia and Central Nigeria (Fig. 3a). Warming ($\geq$1^{o}C) is induced by $CH_4$2 all over the simulation domain; higher warming is induced at northern and eastern part of the simulation domain (Sahara, EGC, ES, Fig. 1b). The areas with relatively higher induced warming are characterised by induced dryness (Figs. 2b and 3b). The $CO_2$2 induced warming of up to 1^{o}C over the ocean and southern countries with higher warming (2-4^{o}C) at the northern countries (Fig. 3c). Similarly, the introduction of N_2O2 led to warming of up to +1^{o}C at the south (EGC, Fig. 1b) and south-eastern part of the simulation domain (southern Chad) is warmer (up to 3^{o}C). This shows the higher potential of N_2O for global warming (Zaehle et al. 2011). The expected

warming due to increased GHGs is simulated generally by the double GHGs experiments. The area dependent nature of response of climate to changes in the level of GHGs is revealed in the experiments with GHGs induced higher warming in some areas of the simulation domain (Fig. 3b-d) (Berntsen, 2006; Lin et al. 1988).With the halved CFC11; slight patches of cooling results at the north, (Fig. 3e) and the induced warming is generally reduced compared to the double greenhouse gases experiment. Halved CFC12 induced similar pattern of temperature change compared to CFC110.5 induced temperature changes (Fig. 3f). This shows how far the reduction in GHGs especially the CFCs can impact global warming. However, warming is induced in larger part of the simulation domain. This is as a result of the combined effect of the other greenhouse gases and the halved CFCs.

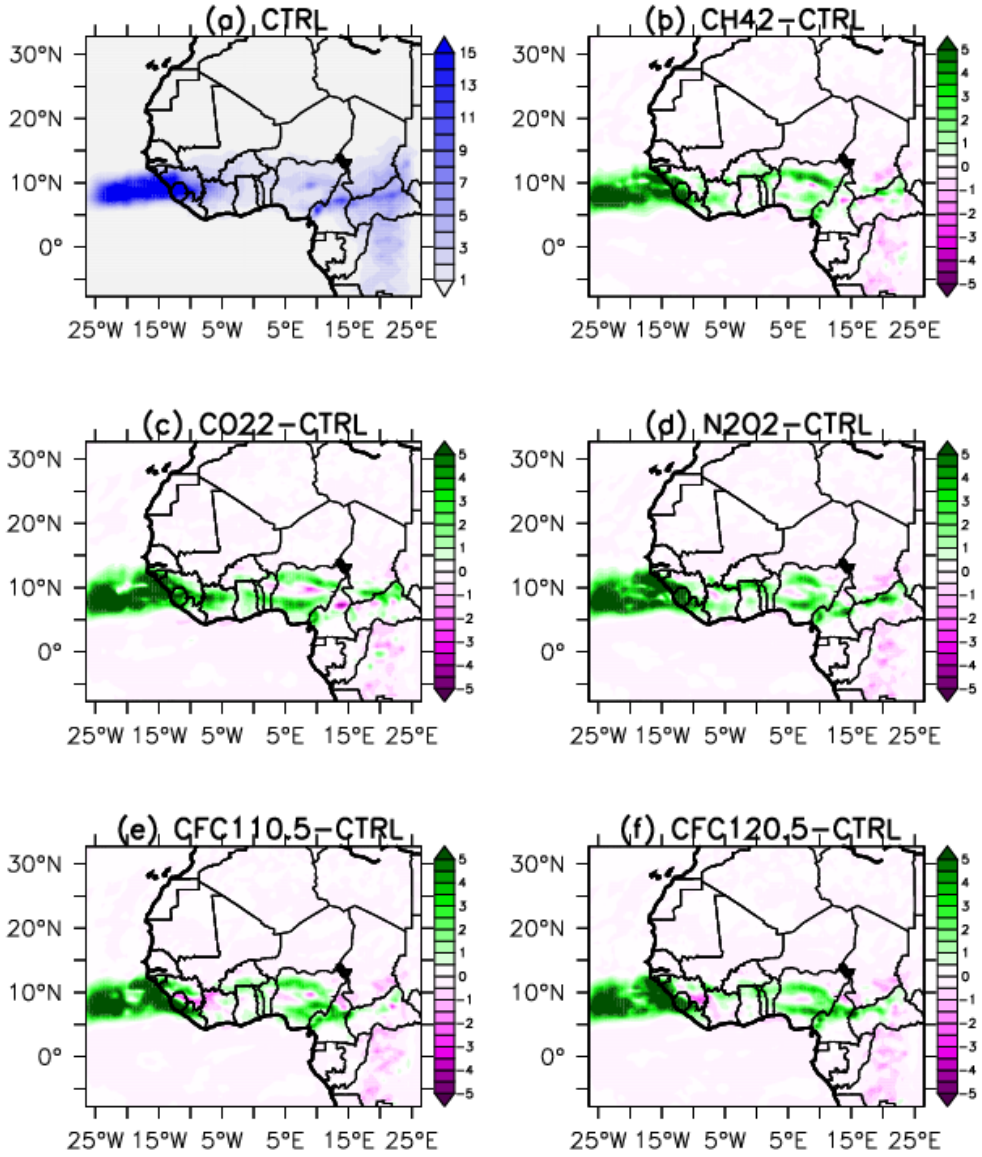

Fig. 2. Simulated JJA precipitation (mm/day) from (a) CTRL, (b) CH_4x2-CTRL, (c) CO_2x2- CTRL, (d) N_2Ox2-CTRL, (e) CFC11x0.5-CTRL and (f) CFC12x0.5-CTRL. The vertical axis represents the latitude, while the horizontal axis is the longitude.

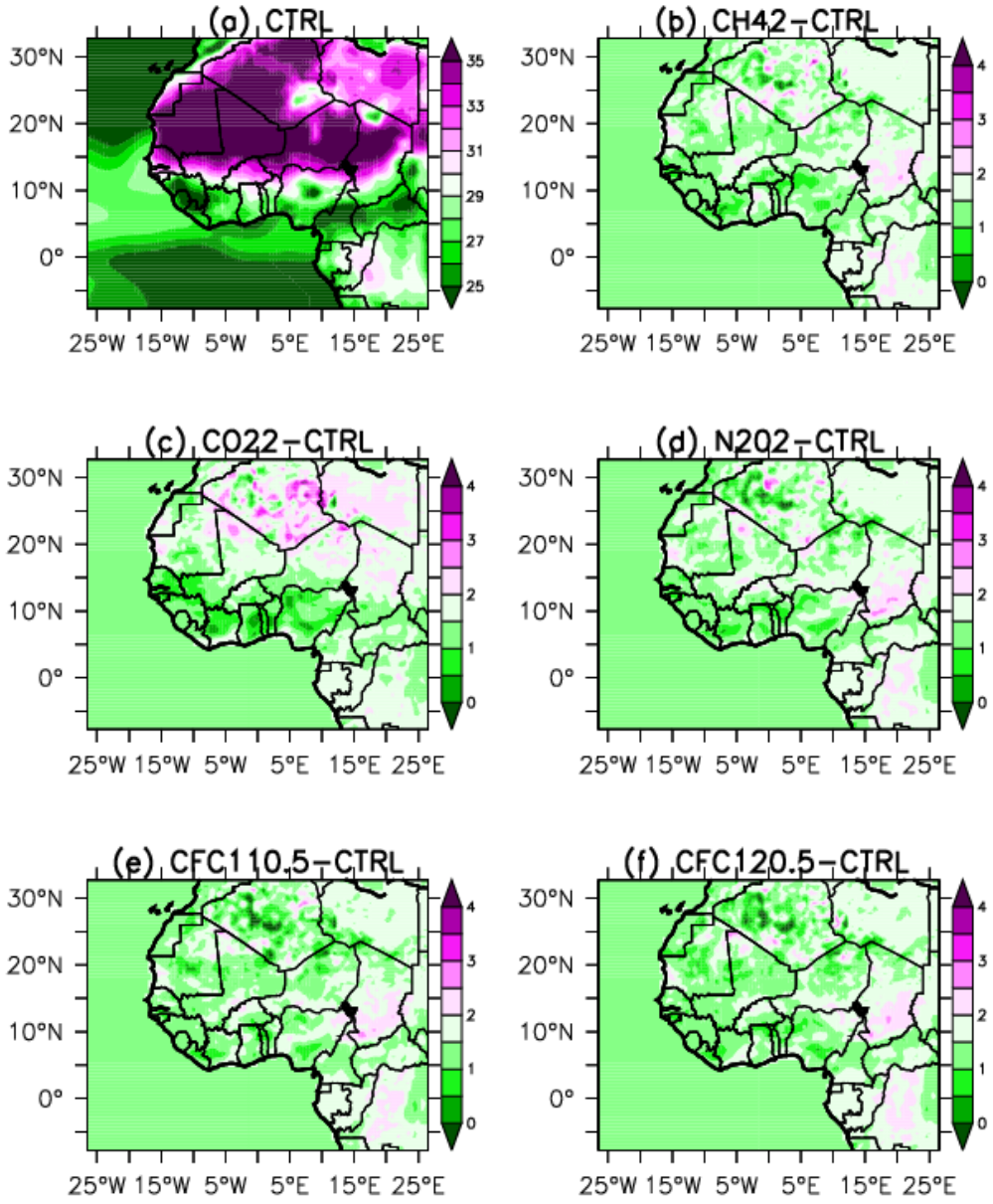

Fig. 3. Simulated JJA ground temperature (^{o}C) (a) CTRL, (b) CH_4x2-CTRL, (c) CO_2x2- CTRL, (d) N_2Ox2-CTRL, (e) CFC11x0.5-CTRL and (f) CFC12x0.5-CTRL. The vertical axis represents the latitude, while the horizontal axis is the longitude.

The simulated specific humidity in the control experiment reduces from the surface to the upper troposphere with more humidity below 15^{o}N (Fig. 4a). The $CH_4$2 induces little or no changes in specific humidity at the upper troposphere. At the lower troposphere (between 1000 and 800 hPa), q increases from 0-12^{o}N up to 12 x 10^{-5} kg/kg with highest increase between 3 and 10^{o}N (Fig. 4b). This corroborates the wetness induced between 5 and 12^{o}N (Fig. 2b-f). Reduction in specific humidity is induced at the mid troposphere by $CH_4$2 between -5 and 0^{o}N (Fig. 4b). This explains the slight reduction induced in precipitation below the equator. $CO_2$2 induced general increase in specific humidity with extended spatial coverage than that induced by $CH_4$2 at the lower troposphere. Slight reduction in specific humidity is induced close to the

equator (-5 to 0°N) at the mid-troposphere (Fig. 4c) but with lower magnitude compared to $CH_4$2 induced reduction at the same location (Figs. 4b, c). N_2O2 induced similar pattern of changes in specific humidity with respect to $CH_4$2 and $CO_2$2 induced changes (Fig. 4b, c, d). The N_2O is less abundant than CH_4 and CO_2 but its potential to influence changes in specific humidity in the atmosphere is relatively higher than the other GHGs, in the sense that it induces comparable changes in relative humidity with respect to CO_2 and CH_4 (Zaehle et al. 2011).

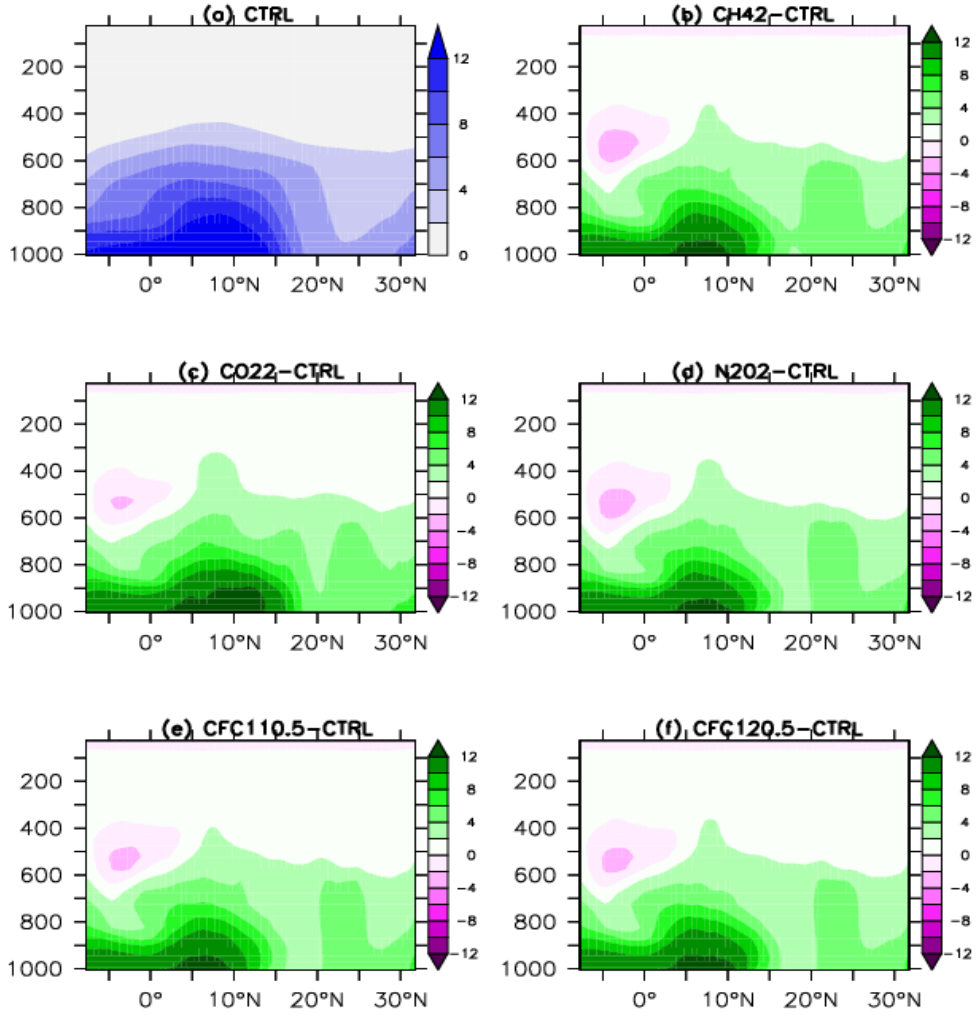

Fig. 4. Simulated zonal mean of JJA specific humidity (a) CTRL (x10^{-4} kg/kg), (b) CH_4x2-CTRL, (c) CO_2x2-CTRL, (d) N_2Ox2-CTRL, (e) CFC11x0.5-CTRL and (f) CFC12x0.5-CTRL. The simulated difference in b, c, d, e and f are displayed in10^{-5} kg/kg. The vertical axis represents the atmospheric pressure levels, while the horizontal axis is the latitude.

Figure 5 shows the profiles of simulated zonal wind from the control experiment (a), the $CH_4$2 induced changes (b), $CO_2$2 induced changes (c), N_2O2 induced changes (d), CFC110.5 induced changes (e), and CFC120.5 induced changes (f) in zonal wind. The simulated zonal wind shows a jet of positive zonal wind centred at 200 hPa and 32°N i.e. the West African westerly jet, Africa Easterly Jet (AEJ) centred at 600 hPa and Tropical Easterly Jet (TEJ) centred at 100 hPa. $CH_4$2 induces a vertical tripole anomaly of jet with easterly anomaly centred at 200 hPa and

westerly anomalies centred at 100 and 500 hPa. Furthermore, two anomalous zonal winds are induced by the double CH_4; negative is centred at 17.5^{o}N and positive at 24^{o}N from the surface to 700 hPa. The negative pole zonal wind anomaly at the surface (15-20^{o}N) in the $CH_4$2 experiment reverses sign in the double CO_2 experiment (Fig. 5b, c), while the positive pole anomaly (25-32^{o}N)extends to the upper atmosphere. $CO_2$2 induces a similar vertical tripole pattern of jet anomaly with respect to $CH_4$2. Anomalies similar to those induced by $CH_4$2 are induced by N_2O2. CFC110.5 and CFC120.5 induce similar changes in the zonal wind compared to $CH_4$2 induced changes, but with weaker changes induced at 200 hPa. The strength of AEJ is reversed while that of TEJ is enhanced (Fig. 5). The induced strength in the jet anomaly at 200 hPa by the double GHGs is most in the $CO_2$2 experiment such that double CO_2 has most influence on wind changes. Wind changes in-turn influence temperature (Fig. 3c) and precipitation (Fig. 2c) changes at different parts of the region (Skinner & Difenbaugh, 2014).

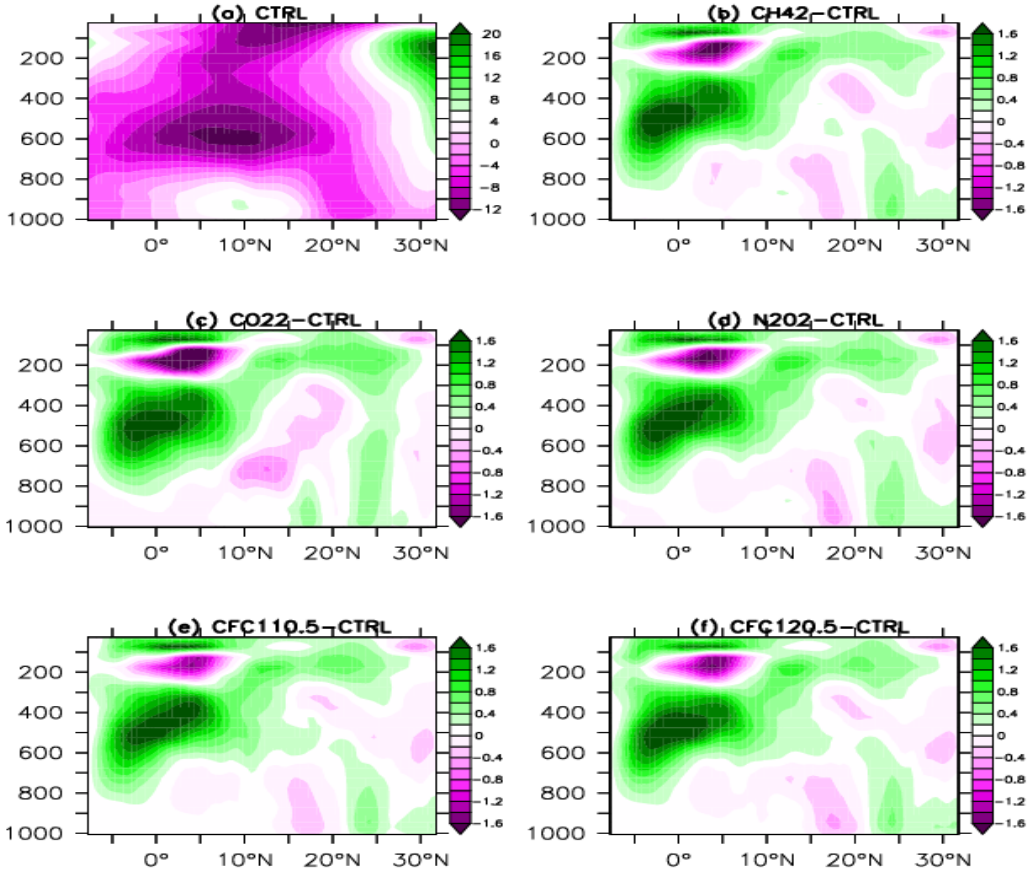

Fig. 5. Simulated zonal mean of JJA zonal wind (m/s) (a) CTRL, (b) CH_4x2-CTRL, (c) CO_2x2-CTRL, (d) N_2Ox2-CTRL, (e) CFC11x0.5-CTRL and (f) CFC12x0.5-CTRL. The vertical axis represents the atmospheric pressure levels, while the horizontal axis is the latitude.

Figure 6 shows the simulated omega in the control experiment (a), induced changes in omega from the $CH_4$2 experiment (b), induced changes in omega from the $CO_2$2 experiment (c), induced changes in omega from the N_2O2 experiment (d), induced changes in omega from the CFC110.5 experiment (e) and induced changes in omega from the CFC120.5 experiment (f). Almost positive omega is simulated over the

simulation domain from the surface to the upper troposphere except from the surface to 600 hPa between 5 and 22^{o}N where negative omega is simulated, which indicate ascent. Double CH_4 experiment induces substantial anomalous ascent (negative omega) at mid-to-upper troposphere between 5 and 13^{o}N latitudes. Insignificant increase in omega is induced at the upper troposphere (Fig 6b). Similar changes in omega are induced by $CO_2$2 experiment but with stronger negative anomaly (ascent) at 7.5^{o}N. Double N_2O2 induced similar omega changes with respect to $CH_4$2 induced changes with extended anomalous ascent to the lower troposphere (Fig. 6d).Double CO_2 experiment induces more anomalous ascent at the lower troposphere than other double GHGs. Halved CFC11 andCFC12 generally induce weakened ascent. Induced positive changes in omega (descent) would lead to reduced convection and precipitation while induced negative change in omega (ascent) would induce convection and precipitation increase at the respective areas. The anomalous ascent induced between 5 and 13^{o}N is in line with the anomalous increase in precipitation induced by the double GHGs (Figs 2 and 6) at the location.

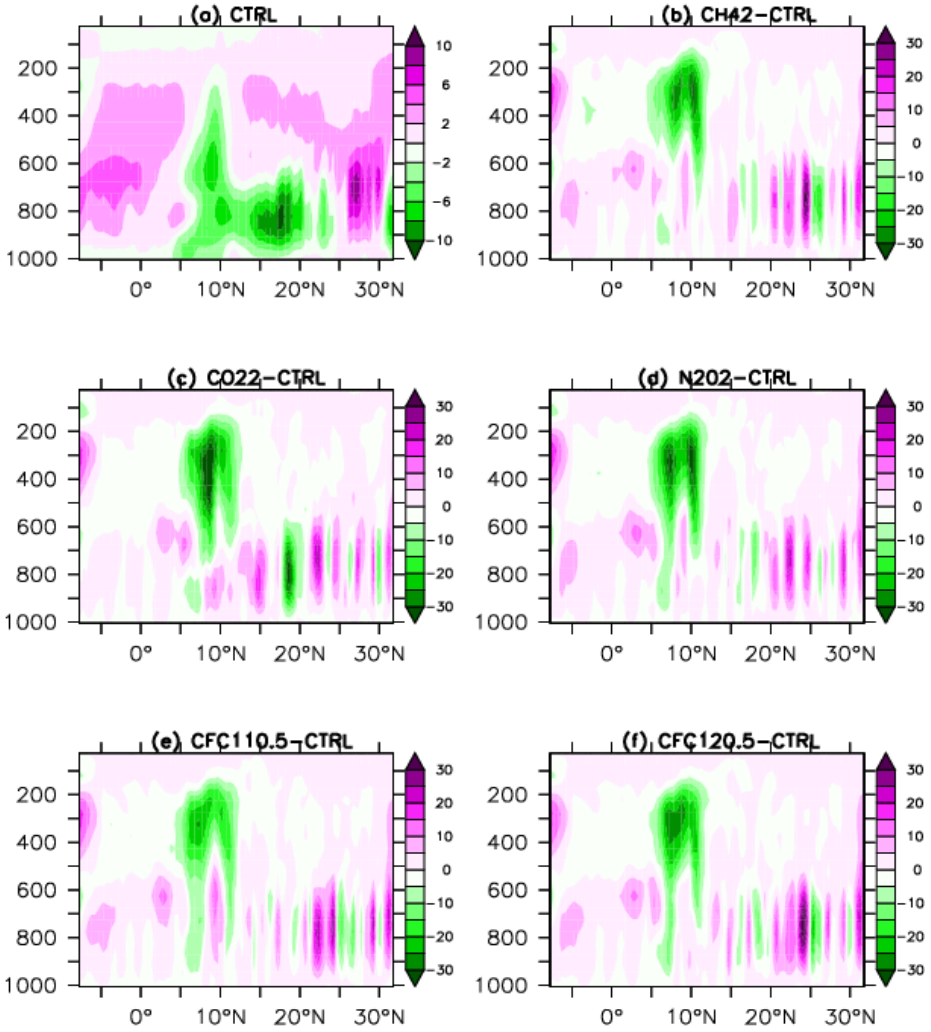

Fig. 6. Simulated zonal mean of JJA omega pressure velocity (a) CTRL (x10^{-4} hPa/s), (b) CH_4x2-CTRL, (c) CO_2x2-CTRL, (d) N_2Ox2-CTRL, (e) CFC11x0.5-CTRL and (f) CFC12x0.5-CTRL. The simulated difference in b, c, d, e and f are displayed in 10^{-5}hPa/s. The vertical axis represents the atmospheric pressure levels, while the horizontal axis is the latitude.

The simulated CLoud Water content (CLW) in control, induced changes in CLW from double and halved greenhouse gases experiments are shown Fig. 7. Simulated CLW in the control experiment is maximum at the lower troposphere and reduces towards the upper troposphere. Little or no CLW is simulated above 15^{o}N The $CH_4$2 induced increase CLW content between 5 an10^{o}N at the lower troposphere which extended to 15^{o}N at the mid troposphere. Reduction in CLW is induced from 400 hPa to upper troposphere between 0 and 15^{o}N. The $CO_2$2 and N_2O2 experiments show similar induced changes in CLW compared to $CH_4$2 induced changes in CLW with only little different spatial extensions (Fig. 6 b, c, d). Halved CFC11induces similar changes as seen in the double GHGs experiments but with weakened increase at the upper troposphere. The induced changes in CLW from the different experiments are significant between the 0 and 15^{o}N and 900 -400 hPa.

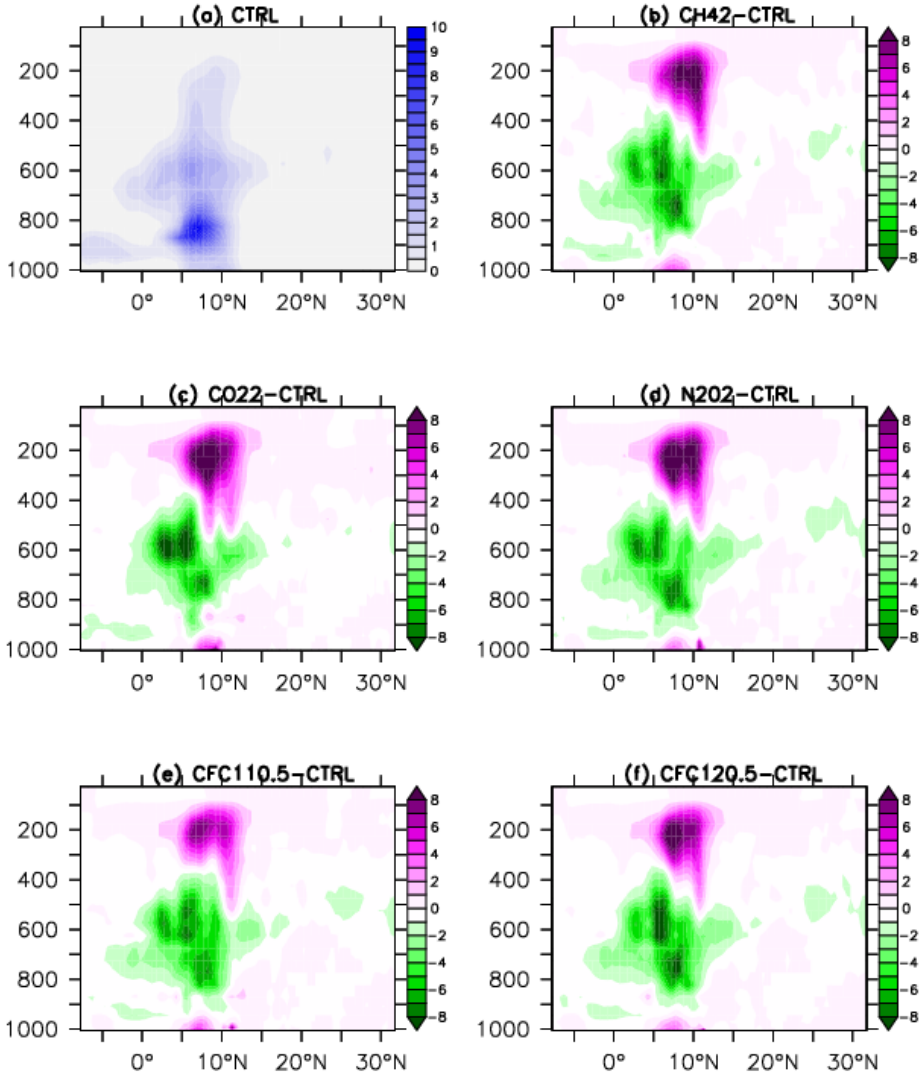

Fig. 7. Simulated zonal mean of JJA cloud water content (a) CTRL (x10^{-5} g/m^2), (b) CH_4x2-CTRL, (c) CO_2x2-CTRL, (d) N_2Ox2-CTRL, (e) CFC11x0.5-CTRL and (f) CFC12x0.5-CTRL. The simulated difference in b, c, d, e, and f are displayed in 10^{-6} g/m^2. The vertical axis represents the atmospheric pressure levels, while the horizontal axis is the latitude.

CONCLUSION

The response of climate of West Africa to changes in the levels of GHGs in the atmosphere was simulated using RegCM4.5. This was done to study the local peculiarities in the effects of GHGs on the climate of West Africa. Double CH_4, CO_2, N_2O and halved CFC11 and CFC12 were used in different experiments. The halved CFC11 and CFC12 induced general reduction in precipitation and lower increase in temperature in larger part of the simulation domain compared to the double GHGs experiments. Reducing the level of CFC11 and CFC12 has little effect on the climate of West Africa, only a limited area has induced dryness and cooling. Double CH_4, CO_2 and N_2O in the atmosphere induce wetter and warmer West Africa in general as expected (Ramanathan & Feng, 2009). However, notable dryness and cooling are induced in specific areas of the simulation domain. Dryness is generally induced at the hilly and mountainous areas of SW Ghana, Central Nigeria, Northern Cameroon, South-eastern Central African Republic. Tripole anomaly of vertical jet, with negative anomaly at 200 hPa and positive anomaly at 100 and 500 hPa is induced by double GHGs. The TEJ is strengthened by double GHGs. In addition, the double GHGs induce dipole of anomaly of zonal wind with positive at the lower latitude and negative at higher latitude at the northern part of West Africa. These induced wind anomalies have consequences on the induced temperature and precipitation over West Africa.

ACKNOWLEDGEMENT

The authors are grateful to the Earth System Physics Research Group at ICTP for the release of RegCM4 model used for this investigation.

REFERENCES

Adams, O. K. (2016). Diversification of Nigeria Economy through Agricultural Production. IOSR-J. Econ. Finan., 7(6); 104-107.

Adeniyi, M. O. (2014). Sensitivity of different convection schemes in RegCM4.0 for simulation of precipitation during the Septembers of 1989 and 1998 over West Africa, Theor. Appl. Climatol., 115(1–2); 305–322.

Adeniyi, M. O. (2016). The consequences of the IPCC AR5 RCPs 4.5 and 8.5 climate change scenarios on precipitation in West Africa, Clim. Change, 139; 245–263.

Anderson, T. R., Hawkins, E. and Jones, P. D. (2016). CO2, the greenhouse effect and global warming: from the pioneering work of Arrhenius and Callendar to today's earth system models. Endeavour, 40(3); 178-187.

Arakawa, A. and Schubert, W. H. (1974). Interaction of a cumulus cloud ensemble with the large-scale environment, Part I. J. Atmos. Sci., 31; 674–701.

Baede, A. P. M., Ahlonsou, E., Ding, Y. and Schimel, D. (2001). Climate system an overview, Bolvin, B. and Pollonas, S. (eds). In: Climate Change (2001: The Scientific Basis. Contribution of Working Group I to the Third Assessment Report of the Intergovernmental Panel on Climate Change [Houghton, J.T., Y. Ding, D. J. Griggs, M. Noguer, P. J. van der Linden, X. Dai, K. Maskell, and C. A. Johnson (eds.)]. Cambridge University Press, Cambridge, United Kingdom and New York, NY, USA; 85-98.

Berntsen, T., Fuglestvedt, J., Myhre, G., Stordal, F. and Berglen, T. (2006). Abatement of greenhouse gases: Does location matter? Clim. Change, 74; 377-411.

Bousquet, P., Ciais P., Miller, J. B., Dlugokencky, E. J. Hauglustaine, D. A., Prigent, C. Van der Werf, G. R., Peylin, P., Brunke, E.-G., Carouge, C., Langenfelds, R. L., Lathière, J. Papa, F., Ramonet, M., Schmidt, M., Steele, L. P., Tyler S. C. and White J. (2006). Contribution of anthropogenic and natural sources to atmospheric methane variability. Nature, 44; 439–443.

Davidson, E. A. and Kanter, D. (2014). Inventories and scenarios of nitrous oxide emissions Environ. Res. Lett., 9; 105012.

Dee, D. P., Uppala, S. M., Simmons, A. J., Berrisford, P., Poli, P., Kobayashi, S., Andrae, U., Balmaseda, M. A., Balsamo, G., Bauer, P., Bechtold, P., Beljaars, A. C. M., van de Berg, L., Bidlot, J., Bormann, N., Delsol, C., Dragani, R., Fuentes, M., Geer., A. J., Haimberger, L., Healy, S. B., Hersbach, H., Ho´lm, E. V., Isaksen, L., Ka°llberg, P., Ko¨hler, M., Matricardi, M., McNally, A. P., Monge-Sanz, B. M., Morcrette, J. –J., Park, B. –K., Peubey, C., de Rosnay, P., Tavolato, C., The´paut, J. –N., d Vitart, F. (2011).

The ERA-interim reanalysis: configuration and performance of the data assimilation system. Quart. J. R. Meteorol. Soc., 137; 553–597.

Emanuel, K. A. (1991). A scheme for representing cumulus convection in large-scale models. J. Atmos. Sci., 48; 2313–2335.

Etminan, M., Myhre, G., Highwood, E. J. and Shine, K. P. (2016). Radiative forcing of carbon dioxide, methane, and nitrous oxide: A significant revision of the methane radiative forcing. Geophys. Res. Lett., 43, 12; 614–12,623.

Hansen, J., Kharecha, P., Sato, M., Masson-Delmotte, V., Ackerman, F., Beerling, D. J., Paul J. Hearty, P. J., Hoegh-Guldberg, O, Hsu S.-L., Parmesan, C., Rockstrom J., Rohling, E. J., Sachs, J., Smith, P. Steffen, K., Van Susteren L., von Schuckmann, K. and Zachos , J. C. (2013). Assessing "Dangerous Climate Change": Required Reduction of Carbon Emissions to Protect Young People, Future Generations and Nature. PLoS ONE 8(12); e81648.

Holtslag, A. A. M., de Bruijn, E. I. F. and Pan, H. L. (1990). A high resolution air mass transformation model for short-range weather forecasting. Mon. Weather Rev., 118; 1561–1575.

Karl, T. R. and Tremberth, K. E. (2003). Modern global climate change. Science, 302(5651); 1719-1723.

Kiehl, J. T., Hack, J. J. Bonan, G. B. Boville, B. A. Williamson, D. L. and Rasch, P. J. (1998). The National Center for Atmospheric Research Community Climate Model: CCM3. JCLI., 11; 1131-1149.

Le Treut, H., Somerville, R., Cubasch, U., Ding,Y., Mauritzen, C., Mokssit, A., Peterson, T. and Prather, M. (2007). Historical overview of climate change science. In Solomon, S., Qin, D., Manning, M., Chen, Z., Marquis, M., Averyt, K. B., Tignor, M. and Miller, H. L.(eds),Climate Change 2007: The physical science basis. Contribution of Working Group I to the Fourth Assessment Report of the Intergovernmental Panel on Climate Change. Cambridge University Press, UK.

Lin, X., Trainer, M. and Liu, S.C. (1988). On the non-linearity of the tropospheric ozone production, J. Geophys. Res., 93; 15, 879–15,888.

McMichael, A. J. (2001). Human frontiers, environments and disease. Cambridge University Press, UK.

Pal, J. S., Small, E. E. and Eltahir, E. A. B. (2000). Simulation of regional-scale water and energy budgets: representation of subgrid cloud and precipitation processes within RegCM. J. Geophys. Res.-Atmos., 105(D24); 29,579–29,594.

Ramanathan, V. and Feng, Y. (2009). Air pollution, greenhouse gases and climate change: global and regional perspectives. Atmos. Environ., 43; 37-50.

Skinner, C. B. and Diffenbaugh, N. S. (2014). Projected changes in African easterly wave intensity and track in response to greenhouse forcing. Proc. Nal. Acad. Sci., USA, 111(19); 6882-6887.

Stainforth, D. A., Allen, M. R., Tredge, E. R. and Smith, L. A. (2007). Confidence, Uncertainty and Decision-Support Relevance in Climate Predictions. Philos. Trans. R. Soc. Lond. A 365; 2145–61.

Strangeways, I. (2011).The greenhouse effect: a closer look. Weather, 66(2); 43-48.

Suberu O. J., Ajala O. A., Akande M. O., Olure-Bank Adeyinka (2015). Diversification of the Nigerian Economy towards a Sustainable Growth and Economic Development. Int. J. Econ., Fin. Man. Sci. 3(2); 107-114.

Watson, R. T. and McMichael, A. J. (2001). Global climate change-the latest assessment: Does global warming warrant a health warning? Global Change Human Health 2; 64–75.

Zaehle, S., Ciais, P., Friend, A. D. and Prieur, V. (2011). Carbon benefits of anthropogenic reactive nitrogen offset by nitrous oxide emissions. Nature Geosci., 4(9); 601-605.

Zeng, X., Zhao, M. and Dickinson, R. E. (1998). Intercomparison of bulk aerodynamic algorithms for the computation of sea surface fluxes using TOGA COARE and TAO data, J. Climatol., 11; 2628–2644.

Zhang, H., Bai, X., Xue, J., Chen, Z., Tang, H. and Chen, F. (2013). Emission of CH4 and N2O under different tillage systems from double-cropped paddy fields in southern China. PLoS One, 8(6); e65277.

Zhuang, Q., Melillo, J. M., Mcguire, A. D., Kicklighter, D. W., Prinn, R. G., Steudler, P. A., Felzer, B. S., and Hu, S. (2007). Net emissions of CH4 and CO2 in Alaska: implications for the region's greenhouse gas budget. Ecol. Appl., 17(1); 203–212.